

Deriving high-resolution velocity maps from low-resolution Fourier velocity encoded MRI data

Vinicius de Carvalho Rispoli (vrispoli@pgea.unb.br)
Joao Luiz Azevedo de Carvalho (joaoluiz@pgea.unb.br)

Department of Electrical Engineering
University of Brasilia, Brasilia-DF, Brasil

Introduction

- ▶ Fourier velocity encoding (FVE) [1] provides considerably higher SNR than phase contrast (PC), and is robust to partial-volume effects.
- ▶ FVE data are typically acquired with low spatial resolution, due to scan-time restrictions.
- ▶ FVE provides the velocity distribution associated with a large voxel, but does not directly provides a velocity map.
- ▶ **Objective:** to propose a method for deriving high-resolution velocity maps from low-resolution FVE data.

Spiral FVE signal model

- ▶ Spiral FVE is a rapid method for FVE-based velocity-distribution measurement [2].
- ▶ The FVE spatial-velocity distribution, $s(x, y, v)$, may be modeled as:

$$s(x, y, v) = \left[m(x, y) \times \text{sinc} \left(\frac{v - v_0(x, y)}{\Delta v} \right) \right] * \text{jinc} \left(\frac{\sqrt{x^2 + y^2}}{\Delta r} \right) \quad (1)$$

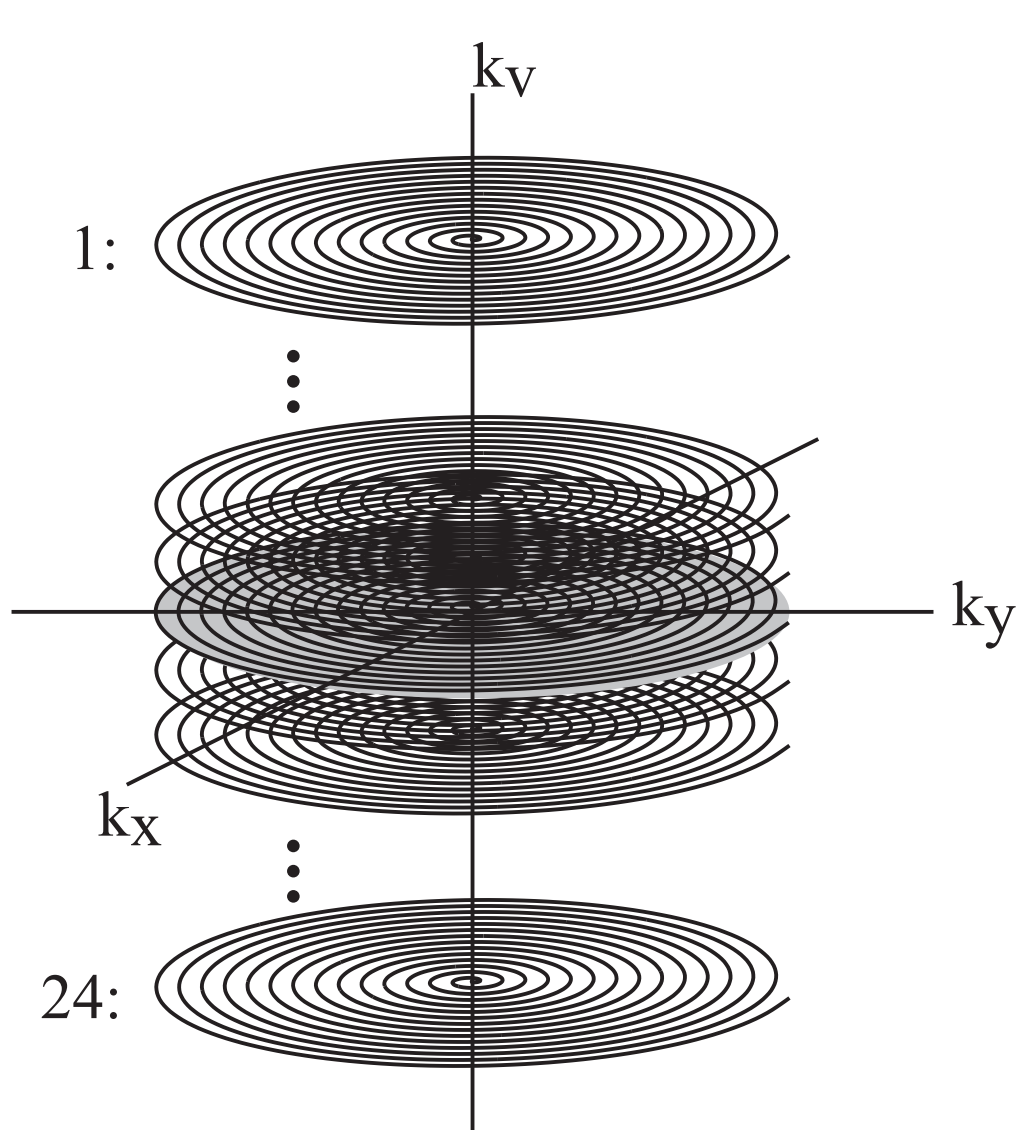


Figure 1: Spiral FVE's k -space coverage consists of a stack-of-spirals in k_x - k_y - k_v [2].

where $m(x, y)$ is the spin-density map; $v_0(x, y)$ is the velocity map; Δv is the FVE velocity resolution; and Δr is the FVE spatial resolution [3].

- ▶ $\text{sinc}(v)$ and $\text{jinc}(r)$ are the blurring kernels associated with the rectangular and circular coverages in k_v and k_x - k_y , respectively (Fig. 1).

Estimating the velocity map

- ▶ The jinc kernel's spatial blurring effects are reduced, using the deconvolution algorithm proposed in ref. [4]. Hence, we obtain:

$$\tilde{s}(x, y, v) \approx m(x, y) \cdot \text{sinc} \left(\frac{v - v_0(x, y)}{\Delta v} \right) \quad (2)$$

- ▶ If a high-resolution spin-density map, $\tilde{m}(x, y)$, is available, the velocity v_0 associated with a given pixel (x_0, y_0) may be estimated from $\tilde{s}(x, y, v)$ as:

$$\tilde{v}_0(x_0, y_0) = \arg \min_v \left\| \frac{\tilde{s}(x_0, y_0, v)}{\tilde{m}(x_0, y_0)} - \text{sinc} \left(\frac{v - v_0}{\Delta v} \right) \right\|_2 \quad (3)$$

Proof of concept

- ▶ **Experiment 1:** Simulated FVE data with 1 mm spatial resolution was derived — using equation (1) — from a numerical phantom: a parabolic velocity map, with 0.33 mm spatial resolution and $m(x, y) = 1$.
- ▶ **Experiment 2:** Simulated FVE data with 1 mm spatial resolution was derived from the through-plane velocity and spin-density maps, measured with 0.33 mm spatial resolution, at the carotid bifurcation of a carotid flow phantom (Fig. 2). A cine gradient-echo 2DFT PC sequence (0.33 mm resolution, 10 NEX, 80 cm/s Venc) was used.

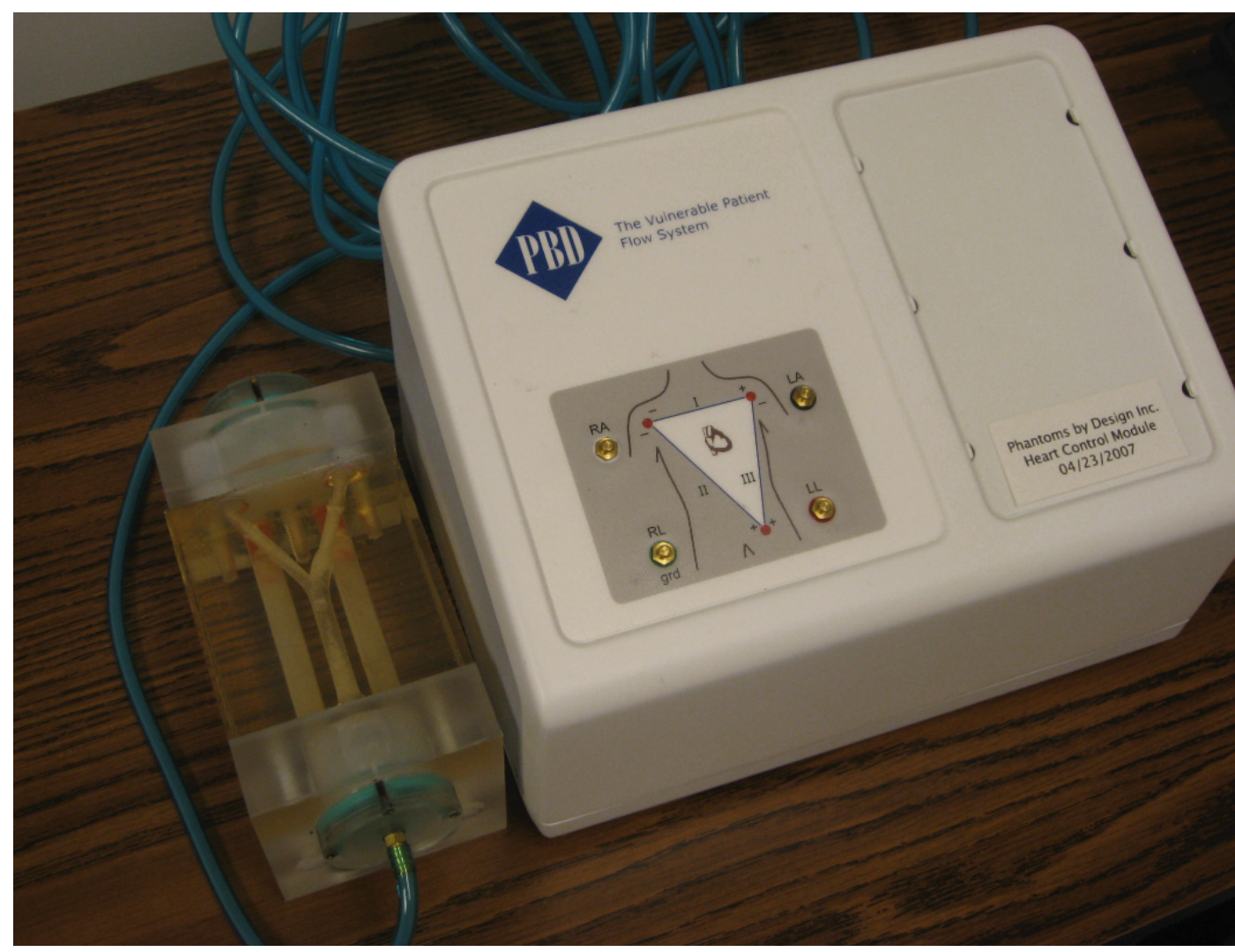


Figure 2: Pulsatile carotid flow phantom (Phantoms by Design, Inc., Bothell, WA).

Results and discussion

- ▶ **Experiment 1:** The velocity map estimated from the simulated low-resolution FVE data was accurate within 3% for the vast majority of the pixels (Fig. 3). This is a very important result, as carotid flow distant to the bifurcation is typically approximately parabolic.
- ▶ **Experiment 2:** The maps estimated from the simulated low-resolution FVE data are very similar (qualitatively) to the reference map (Fig. 4). The error images show that the map obtained using spatial deconvolution (Fig. 4c) was more accurate than the one obtained without spatial deconvolution (Fig. 4b).

Conclusion

- ▶ It is possible to obtain reasonably accurate velocities maps from low-resolution FVE distributions.
- ▶ FVE may potentially be used for driving CFD simulations of carotid flow [5], with considerably higher SNR and robustness to partial voluming than PC MRI.

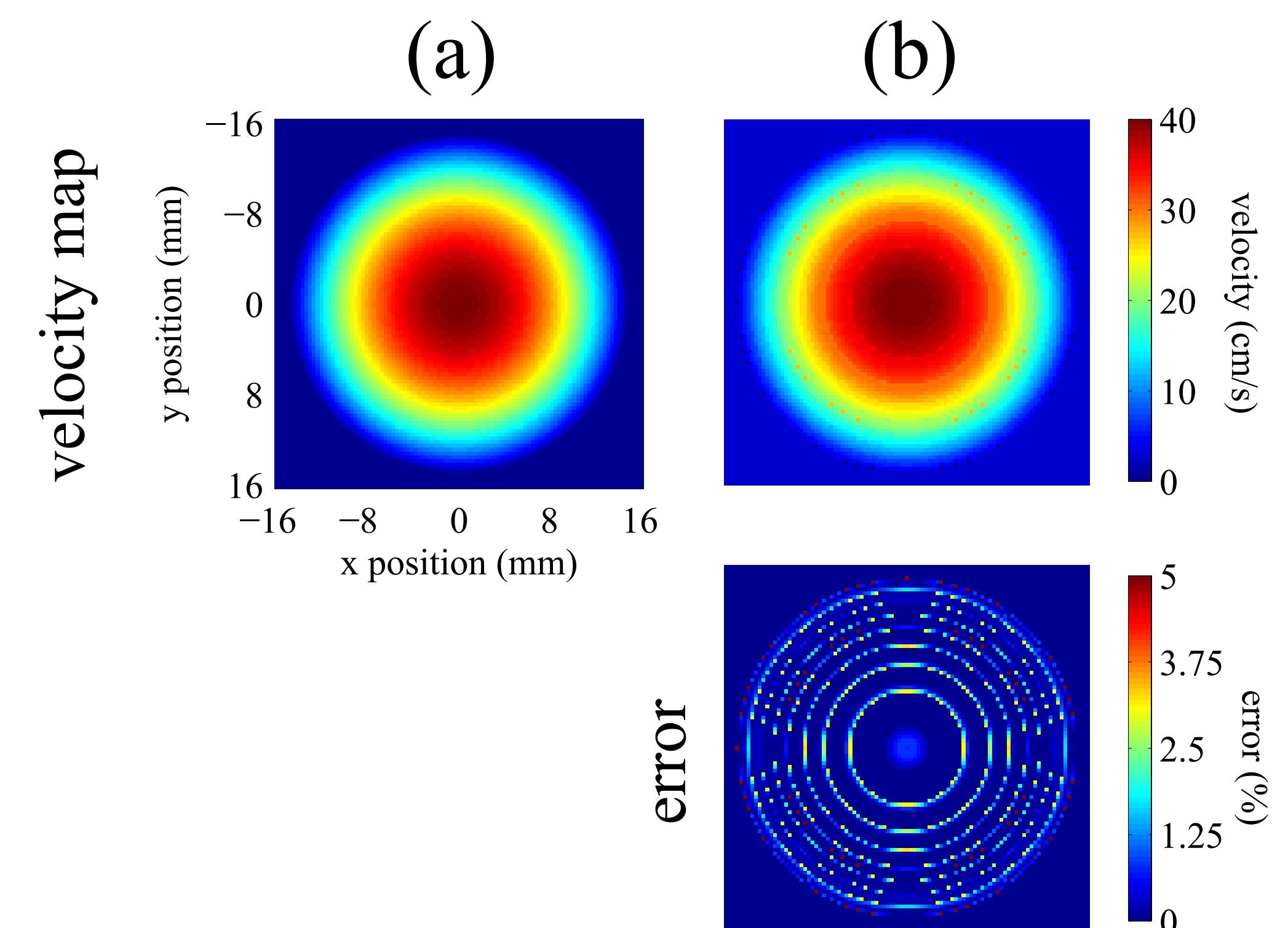


Figure 3: Experiment using a numerical phantom of parabolic flow: (a) reference velocity map; (b) velocity map estimated from the simulated low-resolution FVE data, and associated error percentages.

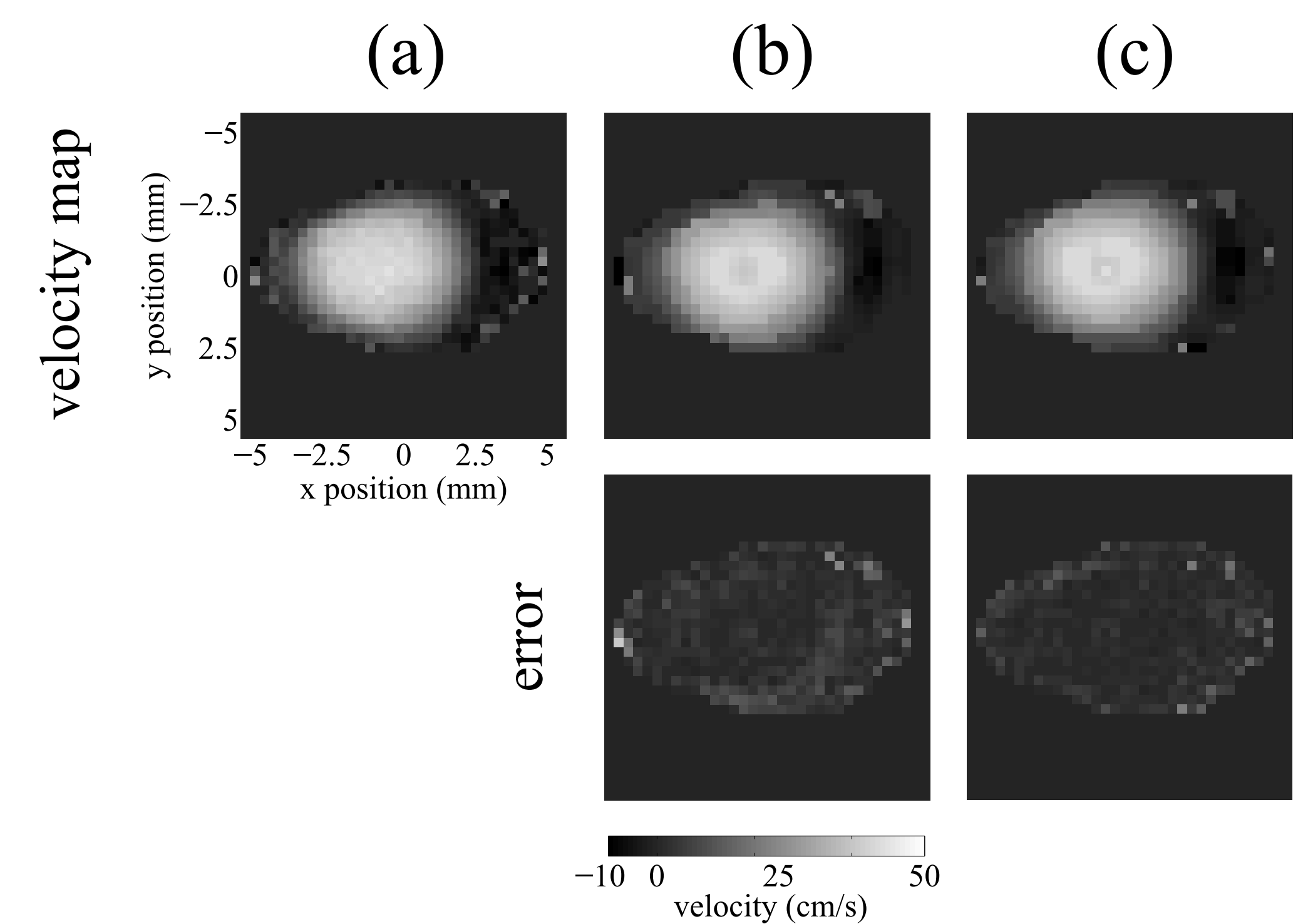


Figure 4: Experiment using the pulsatile carotid flow phantom: (a) reference PC velocity map, measured at the phantom's bifurcation; (b) velocity map estimated from the simulated low-resolution FVE data, without spatial deconvolution (and associated error percentages); and (c) velocity map estimated from the simulated low-resolution FVE data, with spatial deconvolution (and associated error percentages).

References

- [1] Moran PR. MRI 1:197, 1982.
- [2] Carvalho JLA and Nayak KS. MRM 57:639, 2007.
- [3] Carvalho JLA, et al. MRM 63:1537, 2010.
- [4] Krishnan D and Fergus R. Proc 24th NIPS, 2009.
- [5] Nielsen J-F and Nayak KS. Proc ISMRM 17: 3858, 2009.

Financial support

- ▶ Edital DPP/UnB 10/2011